24th INTERNATIONAL CONGRESS ON SOUND AND VIBRATION
23–27 July 2017, London

RECONSTRUCTION OF PARTICLE VELOCITY FIELD AND SOUND PRESSURE FIELD ON THE SOURCE SURFACE BY JOINTLY UTILIZING PARTIAL SOUND PRESSURE AND NORMAL VELOCITY

Zhu Haichao, Mao Rongfu, Su Changwei, Su Junbo and Zhao Yinglong

National Key Laboratory on Ship Vibration and Noise, Naval University of Engineering, Wuhan, China
email: haiczhu@163.com

In order to reduce the number of velocity measurement points, a method of jointly utilizing sound pressure and normal velocity is proposed in this paper to reconstruct particle velocity field and sound pressure field on the source surface. Firstly, a novel form of pressure acoustic radiation modes is derived, which are corresponding with the complex velocity acoustic radiation modes. On this basis, partial sound pressures and normal velocities can be jointly utilized to reconstruct the particle velocity field and the sound pressure field. Finally, numerical simulation on a simple supported plate and experimental verification on a clamped plate are carried out. The results show that the reconstruction can be realized by jointly utilizing partial sound pressures and normal velocities. So we can reduce the number of velocity measurement points by replacing them with sound pressure measurement points. The proposed method is helpful for engineering application of acoustic source identification and acoustic field prediction using partial measurements on the surface of acoustic source.

Keywords: pressure acoustic radiation mode; sound pressure; normal velocity; jointly utilization; reconstruction

1. Introduction

Acoustic source identification and acoustic field prediction have become advanced research hotspots in acoustic field. In recent years, with the development of near-field acoustic holography (NAH) technology, in-depth studies have been made in above two areas. As the name implies, NAH solves acoustic problems by using near-field measurements. However, NAH can only be applied in laboratory as a result of its strict requirements on background noise and sensor position [1]. By contrast, it's simpler and more direct to use measurement data on the source surface to solve these acoustic problems. In general, the more measurement data we know, the higher accuracy of identification and prediction can be achieved. But in practice, it's difficult to place a large number of sensors. Furthermore, if a large number of sensors are arranged on the source surface to measure normal velocity, the vibration of the source will be changed, as a result it will reduce the accuracy of identification and prediction, even cause failure. Hence, how to realize the reconstruction of particle velocity field and sound pressure field on the source surface under the condition of sparse measurement points, especially under the consideration of reducing the number of normal velocity measurement points, is a urgent problem to be solved. In this paper, in order to solve the problem, a novel method of jointly utilizing partial sound pressure and normal velocity on the source surface is proposed based on the acoustic radiation mode (ARM) theory.

ARMs are sets of independently radiating velocity distributions. Since the ARM theory is appeared, the form of ARM keeps changing. Sarkissian [2] firstly put forward the ARM with real vector form (real ARM for short) by an eigen-decomposition of radiation resistance matrix. It is known

to be a powerful tool for interpreting sound radiation since it is easy to calculate and only dependent on geometrical information. A number of scholars developed its theory and application at around the same time, for example, Cunfare [3] and Elliott [4]. At present, the ARM-based methods of acoustic source identification are all based on real ARM. But this real ARM is subject to certain limitations, i.e., in order to calculate the real ARM, the discretization of the source surface must be evenly. It is difficult for the sound sources with complex shapes. With the emergences of multi-level fast multipole algorithm (MLFMA) and preprocessing FFT algorithm, the eigen-decomposition of large matrix can be realized. On this basis, Wu put forward the ARM with complex vector form (complex ARM for short) by an eigen-decomposition of radiation impedance matrix [5]. Obviously, this complex ARM has better applicability on the sound sources with complex shapes.

The work in this paper is based on the complex ARM. For the sake of jointly utilizing sound pressures and normal velocities, a novel form of pressure acoustic radiation mode (p-ARM for short) is derived in Section 2, and the mode is one-to-one corresponding with the complex velocity acoustic radiation mode (v-ARM for short). On this basis, a reconstruction formula, which jointly utilizing partial sound pressures and normal velocities to reconstruct the particle velocity field and the sound pressure field, is established in Section 3. And then, a numerical simulation and an experimental verification are carried out respectively in Section 4 and Section 5, and the feasibility of the method proposed here is verified.

2. Theory of complex ARM

2.1 Complex v-ARM

Dividing the source surface into a number of elementary radiators, and the acoustic power radiated by this array of elementary radiators may be written as

$$\boldsymbol{W} = 1/2\,\mathrm{Re}[\boldsymbol{v}_n{}^H \boldsymbol{S}\boldsymbol{Z}\boldsymbol{v}_n], \tag{1}$$

where $\boldsymbol{S}$ is a diagonal matrix, its diagonal elements are the areas of the elementary radiators Δs_i. $\boldsymbol{Z}$ is the radiation impedance matrix. $\boldsymbol{v}_n$ is the vector of normal velocities at these elementary radiators. Here, conducting an eigen-decomposition on $\boldsymbol{Z}$ directly, that can be written as

$$\boldsymbol{Z} = \boldsymbol{\Phi}\boldsymbol{\Lambda}\boldsymbol{\Phi}^H, \tag{2}$$

in which $\boldsymbol{\Phi}$ is an unitary matrix of eigenvectors, and its columns $\boldsymbol{\varphi}_i (i = 1, 2, \cdots N)$ are v-ARMs which have complex vector forms. $\boldsymbol{\Lambda} = diag[\lambda_1, \lambda_2, ..., \lambda_i, ...]$ is a diagonal matrix of eigenvalues λ_i. The vector of normal velocities at these elementary radiators on the source surface is the sum of the v-ARM amplitudes weighted by the v-ARM shapes, so that

$$\boldsymbol{v}_n = \boldsymbol{\Phi}\boldsymbol{c}, \tag{3}$$

in which $\boldsymbol{c}$ is the vector of v-ARM amplitudes. Substituting Eq. (2) and Eq. (3) into Eq. (1), the acoustic power radiated by this array of elementary radiators can thus be written as

$$\boldsymbol{W} = \sum_{i=1}^{N} \mathrm{Re}(\lambda_i) |c_i|^2 \Delta s_i. \tag{4}$$

It can be seen from Eq. (4), the expression of the acoustic power expressed by the complex v-APM has the same form as that expressed by the real v-ARM. It is important to note that only the real component of λ_i is used to calculate the acoustic power. Based on this, we rearrange the eigenvectors according to the size of the real component of the eigenvalue, i.e., $\mathrm{Re}(\lambda_i)$. Then a set of complex ARMs whose radiation efficiencies ranking from high to low can be obtained, we mark this sorted matrix of complex ARMs as $\boldsymbol{\Phi}_{re}$.

2.2 Complex p-ARM

So far, there is less study on the p-ARM. Berkhoff derived the real p-ARM theory by an eigen-decomposition of the admittance matrix (which is the inverse of $\boldsymbol{Z}$) [6]. In this subsection, it is shown that a complex p-ARM can be obtained by the complex v-ARM calculated above, and the corresponding relations between the p-ARMs and the v-ARMs can also be found.

As we point out in the preface, ARMs are sets of independently radiating velocity distributions. If the acoustic source is vibrating only by the ith ARM, i.e., $\boldsymbol{v}_n=\boldsymbol{\varphi}_i$, then the vector of complex sound pressures immediately in front of each radiator, i.e., $\boldsymbol{p}$ is given by

$$\boldsymbol{p}=\boldsymbol{Z}\boldsymbol{\varphi}_i=\lambda_i\boldsymbol{\varphi}_i, \tag{5}$$

in which λ_i is the eigenvalue corresponding to the eigenvector $\boldsymbol{\varphi}_i$. Obviously, $\lambda_i\boldsymbol{\varphi}_i(i=1,...,N)$ is also a set of basis in vector space, and the set of basis is one-to-one corresponding with the complex v-ARM. So we define this set of basis as the complex pressure acoustic radiation mode, i.e., complex p-ARM. Furthermore, the complex p-ARM and the complex v-ARM have similar form. They are one-to-one corresponding, and there is only a different coefficient between them. It provides a theoretical basis for jointly utilizing sound pressures and normal velocities to solve acoustic problems.

3. Jointly utilize partial sound pressure and normal velocity

According to the above derivation, the vector of normal velocities on the source surface can be expressed by the complex v-ARM expansions

$$\boldsymbol{v}_n=\boldsymbol{\Phi}_{re}\boldsymbol{c}. \tag{6}$$

Combining with the Eq. (5), the vector of complex sound pressures on the source surface can be written as

$$\boldsymbol{p}_s=\boldsymbol{\Phi}_{re}\boldsymbol{\Lambda}_{re}\boldsymbol{c}, \tag{7}$$

in which $\boldsymbol{\Lambda}_{re}$ is the diagonal matrix of sorted eigenvalues.

Assuming that we divide the source surface into N elementary radiators, we can calculate N order ARMs. As the Eq. (6) is characterized by its fast convergence, therefore, the vector of normal velocities and the vector of sound pressures can be represented by a finite numbers of ARMs, i.e., modal truncation. Here, we assume that the cut-off order number of ARMs is N_1, then Eq. (6) and Eq. (7) can be written as

$$\boldsymbol{v}_n\approx\boldsymbol{\Phi}_{re(N\times N_1)}\boldsymbol{c}_{(N_1\times 1)}, \tag{8}$$

$$\boldsymbol{p}_s\approx\boldsymbol{\Phi}_{re(N\times N_1)}\boldsymbol{\Lambda}_{re(N_1\times N_1)}\boldsymbol{c}_{(N_1\times 1)}, \tag{9}$$

where $\boldsymbol{\Phi}_{re(N\times N_1)}$ is a $N\times N_1$ matrix, $\boldsymbol{c}_{(N_1\times 1)}$ is a $N_1\times 1$ vector, $\boldsymbol{\Lambda}_{re(N_1\times N_1)}$ is a $N_1\times N_1$ diagonal matrix. If we have known partial normal velocities on N_2 elements and partial sound pressures on N_3 elements, based on Eq. (8) and Eq. (9), the equations composed by the known data can be written as

$$\boldsymbol{v}_{nk}=\boldsymbol{\Phi}'_{re(N_2\times N_1)}\boldsymbol{c}_{(N_1\times 1)}, \tag{10}$$

$$\boldsymbol{p}_{sk}=\boldsymbol{\Phi}'_{re(N_3\times N_1)}\boldsymbol{\Lambda}_{re(N_1\times N_1)}\boldsymbol{c}_{(N_1\times 1)}. \tag{11}$$

It can be seen that there is a common unknown in the two equations, i.e., the vector of ARM amplitudes $\boldsymbol{c}_{(N_1\times 1)}$. Thus, the simultaneous equations can be constituted by combining Eq. (10) with Eq. (11), then we can solve $\boldsymbol{c}_{(N_1\times 1)}$ by jointly utilizing sound pressures and normal velocities, which is written as

$$\boldsymbol{c}_{(N_1\times 1)}=\begin{bmatrix}\boldsymbol{\Phi}'_{re(N_2\times N_1)}\\ \boldsymbol{\Phi}'_{re(N_3\times N_1)}\boldsymbol{\Lambda}_{re(N_1\times N_1)}\end{bmatrix}^{+}\begin{bmatrix}\boldsymbol{v}_{nk}\\ \boldsymbol{p}_{sk}\end{bmatrix}, \tag{12}$$

in which the superscript $^{+}$ denotes the pseudo-inverse of matrix. And then, substituting the solved $\boldsymbol{c}_{(N_1\times 1)}$ into Eq. (8) and Eq. (9), the particle velocity field and the sound pressure field on the source surface can be reconstructed, which are written as

$$\boldsymbol{v}_n=\boldsymbol{\Phi}_{re(N\times N_1)}\begin{bmatrix}\boldsymbol{\Phi}'_{re(N_2\times N_1)}\\ \boldsymbol{\Phi}'_{re(N_3\times N_1)}\boldsymbol{\Lambda}_{re(N_1\times N_1)}\end{bmatrix}^{+}\begin{bmatrix}\boldsymbol{v}_{nk}\\ \boldsymbol{p}_{sk}\end{bmatrix}, \tag{13}$$

$$\boldsymbol{p}_s=\boldsymbol{\Phi}_{re(N\times N_1)}\boldsymbol{\Lambda}_{re(N_1\times N_1)}\begin{bmatrix}\boldsymbol{\Phi}'_{re(N_2\times N_1)}\\ \boldsymbol{\Phi}'_{re(N_3\times N_1)}\boldsymbol{\Lambda}_{re(N_1\times N_1)}\end{bmatrix}^{+}\begin{bmatrix}\boldsymbol{v}_{nk}\\ \boldsymbol{p}_{sk}\end{bmatrix}. \tag{14}$$

Therefore, we can realize acoustic source identification and acoustic field prediction by jointly utilizing partial sound pressure and normal velocity on the source surface, and the goal to reduce the number of normal velocity measuring points is achieved.

4. Numerical simulation

In this section, we specialize the problem. The system chosen is a simply-supported baffled plate system. The plate is assumed to be made of steel, and its dimensions are $L_x\times L_y\times h$=0.5m×0.5m×0.008m. In the simulation a harmonic point force is located at (x_0, y_0)=(0.125, 0.125), relative to the centre of the plate. The amplitude of the point force is 1N, and the frequency of the point force is 612Hz (equal to the modal frequency of (2, 2) mode). We divide the plate surface into 32×32 elementary radiators. According to the theory given in the Ref. 7, the vector of particle normal velocities on the plate surface can be calculated. Then, the vector of complex sound pressures on the plate surface can be obtained by

$$\boldsymbol{p}_s=\boldsymbol{Z}\boldsymbol{v}_n, \tag{15}$$

where, for radiators in a baffle, the concrete form of the radiation impedance matrix $\boldsymbol{Z}$ is given in the Ref. 6. We mark $\boldsymbol{v}_n$ and $\boldsymbol{p}_s$ calculated by this way as theoretical values. Figure 1 shows the theoretical particle normal velocity and the theoretical sound pressure on the plate surface, each of which contains amplitude and phase.

Now, in order to validate the feasibility and effectiveness of jointly utilizing partial sound pressure data and normal velocity data on the source surface to reconstruct the particle velocity field and the sound pressure field, we consider three different example cases here. The numbers and distributions of measurement points arranged in these cases are introduced, as follows:

In case 1, 25 velocity measurement points and 25 pressure measurement points are arranged evenly, and these distributions are shown in Fig. 2.

In case 2, replacing the 25 pressure measurement points in Fig. 2(b) with 25 velocity measurement points, that's to say, 50 velocity measurement points are arranged.

In case 3, removing the 25 pressure measurement points in Fig. 2(b), that's to say, only 25 velocity measurement points in Fig. 2(a) are arranged.

Next, the particle velocity field and the sound pressure field on the plate surface are reconstructed in three different cases, marking these results as reconstructed values. To compare the differences between theoretical values and reconstructed values, we define error formula as

$$Error=\sqrt{\sum_{i=1}^{N}|v_{ri}-v_{ti}|^2/\sum_{i=1}^{N}|v_{ti}|^2}\times 100\%, \tag{16}$$

in which v_{ri} represents reconstructed values and v_{ti} represents theoretical values. Table 1 lists the reconstruction errors for cases 1, 2 and 3, each of them contains the reconstruction error of velocity

and the reconstruction error of pressure. Here, to save space, we just display the distribution of the normal velocity and the sound pressure reconstructed under case 1, as shown in Fig. 3.

Comparing these results, we can deduce the following conclusions:

(a) Comparing Fig. 3 with Fig. 1, it can be seen that the particle velocity field and the sound pressure field on the plate surface are reconstructed accurately by jointly utilizing partial sound pressure data and normal velocity data.

(b) As shown in Table 1, the reconstruction errors under case 1 are similar to those under case 2. It can be seen that the reconstruction results by jointly utilizing 25 sound pressures and 25 normal velocities are in good agreement with that by directly utilizing 50 normal velocities. So we can find that, by the method proposed in Section 3, the roles of the two types of measurement points, i.e., velocity measurement points and pressure measurement points, are basically the same. That's to say, by this method, we can replace partial velocity measurement points with pressure measurement points. It may have many potential advantages in engineering application.

(c) Comparing the reconstruction errors under case 1 with those under case 3, we can find that, too little number of measurement points results in worse reconstruction result. So jointly utilizing partial sound pressure data and normal velocity data for reconstruction is very necessary.

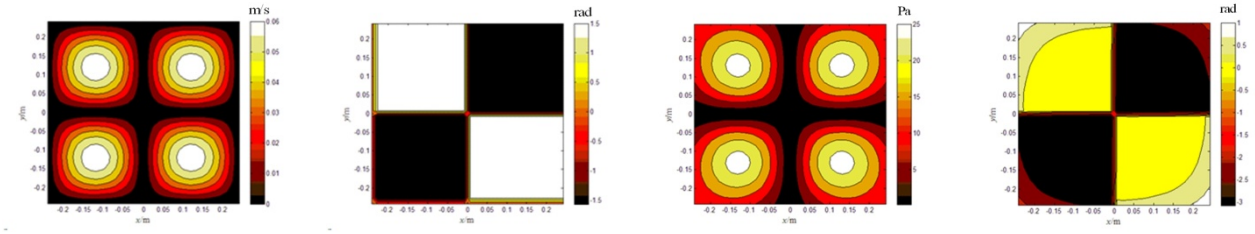

(a) (b) (c) (d)

Figure 1: Theoretical values on the plate surface: (a) Amplitude of normal velocity; (b) Phase of normal velocity; (c) Amplitude of sound pressure; (d) Phase of sound pressure.

(a) (b)

Figure 2: The distributions of measurement points: (a) Velocity measurement points; (b) Pressure measurement points.

Table 1: Reconstruction errors

	Case 1	Case 2	Case 3
Reconstruction error of $\boldsymbol{v}_n$	11.42%	12.23%	20.71%
Reconstruction error of $\boldsymbol{p}_s$	3.01%	5.18%	9.50%

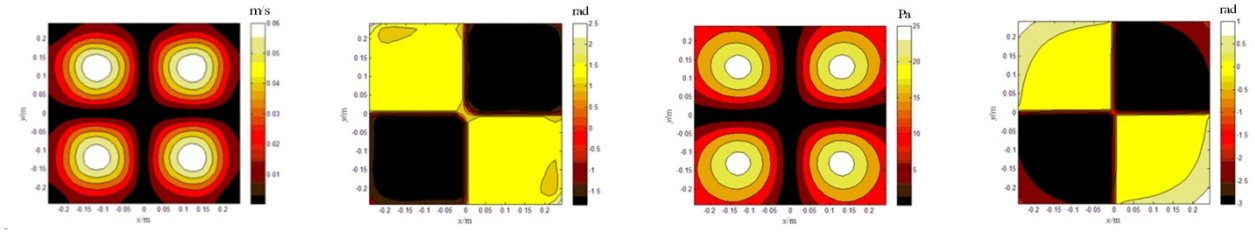

(a) (b) (c) (d)

Figure 3: Reconstructed values on the plate surface under case 1: (a) Amplitude of normal velocity; (b) Phase of normal velocity; (c) Amplitude of sound pressure; (d) Phase of sound pressure.

5. Experimental verification

To further investigate the feasibility of the method proposed in this paper, an experimental verification is carried out. The model chosen here is a clamped rectangular plate. The plate is made of steel, and its dimensions are $L_x \times L_y \times h = 0.5\text{m} \times 0.5\text{m} \times 0.001\text{m}$. The experimental scene is shown as Fig. 4.

It's necessary to note that, we measure the reference values on the plate surface by using NAH technology here. The specific process is as follows: First, using the NAH measurement system to measure the sound pressures on the hologram; Then, the normal velocity and sound pressure on the plate surface, can be reconstructed by NAH technology. The distance between two adjacent measuring points is 0.05m in both two directions, and the distance between the measuring plane and the plate surface is 0.04m .

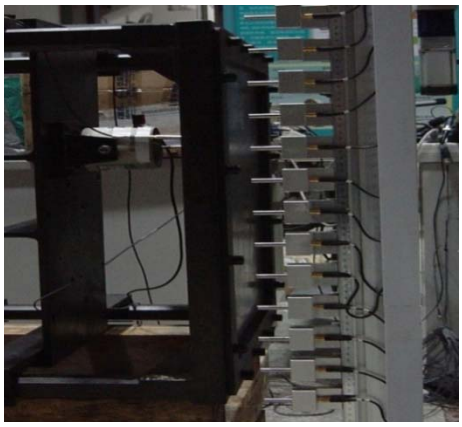

Figure 4: The scene of experiment.

A single point force inertia actuator is used as the disturbance and the forcing frequency is 292Hz (equal to the modal frequency of (3, 3) mode). By stepping the linear array, we get sound pressures on 13×13 near-field measurement points. Then, these measurements can be used to reconstruct the 13×13 normal velocities and 13×13 sound pressures on the plate surface by using NAH technology. Here, mark the results as reference values, as shown in Fig. 5.

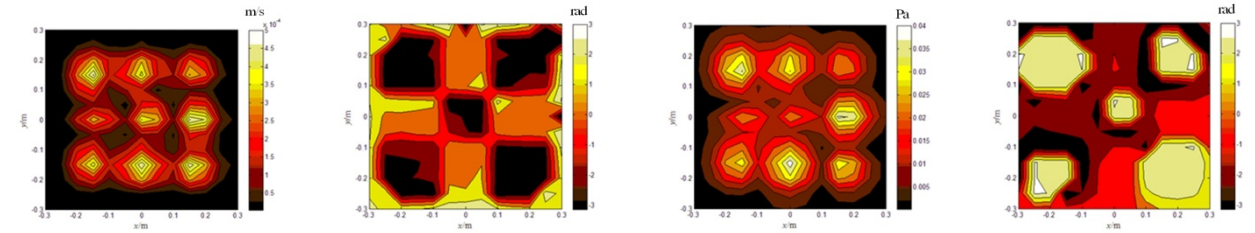

(a) (b) (c) (d)

Figure 5: Reference values on the plate surface: (a) Amplitude of normal velocity; (b) Phase of normal velocity; (c) Amplitude of sound pressure; (d) Phase of sound pressure.

Next, based on the theory introduced in Section 2 and Section 3, we just select 20 normal velocities and 20 sound pressures among the reference values to reconstruct the particle velocity field and the sound pressure field on the plate surface. In other words, there are 20 velocity measurement points and 20 pressure measurement points are arranged evenly on the plate, and these distributions are shown in Fig. 6. By calculating, the reconstruction error of normal velocity is 24.62% and the reconstruction error of sound pressure is 14.38%. The reconstructed results are shown in Fig. 7. Comparing Fig. 7 with Fig. 5, it can be seen that the reconstruction results by jointly utilizing 20 sound pressures and 20 normal velocities are in good agreement with the reference values. So the feasibility of jointly utilizing partial sound pressure data and normal velocity data on the source surface to reconstruct the particle velocity field and the sound pressure field is further verified by this experiment.

(a) (b)

Figure 6: The distributions of measurement points: (a) Velocity measurement points; (b) Pressure measurement points.

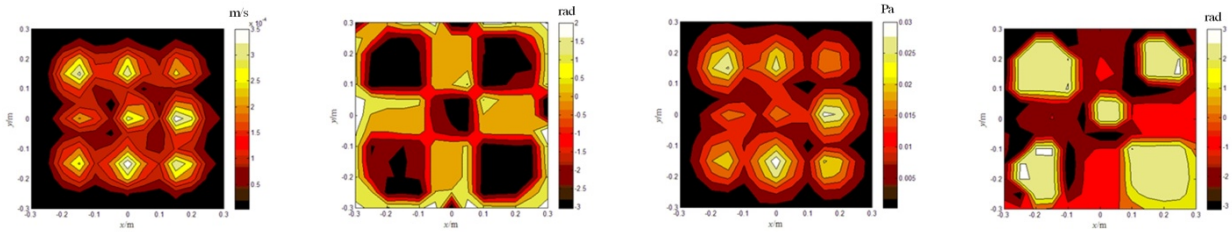

(a) (b) (c) (d)

Figure 5: Reconstructed values on the plate surface: (a) Amplitude of normal velocity; (b) Phase of normal velocity; (c) Amplitude of sound pressure; (d) Phase of sound pressure.

6. Conclusions

In this paper, a method to jointly utilize sound pressure data and normal velocity data on the source surface is proposed for the reconstruction of particle velocity field and sound pressure field. Firstly, a novel form of p-ARM is derived on the basis of the complex v-ARM. Then, with the one-to-one corresponding relationships between the two ARMs, a reconstruction formula of jointly utilizing partial sound pressures and normal velocities is established. And then a numerical simulation on a simple supported plate is carried out, the results show that the particle velocity field and the sound pressure field on the plate surface can be reconstructed accurately by jointly utilizing partial sound pressure data and normal velocity data. Finally, an experimental verification on a clamped plate is carried out, and the feasibility of the method is further verified.

Compared with the traditional methods, this method can realize the reconstruction by jointly utilizing partial sound pressures and normal velocities on the source surface. So we can reduce the number of velocity measurement points by replacing them with sound pressure measurement points, and sometimes take full advantage of the sound pressure data that we had known. Therefore, this

study can promote the engineering application of acoustic source identification and acoustic field prediction while using partial measurements on the surface of acoustic source.

Acknowledgments

The authors gratefully thank the supports from National Natural Science Foundation of China (grants No. 51675529), and express their thanks to the referees for their review of this manuscript.

REFERENCES

1 Gerard P. Carroll. The effect of sensor placement errors on cylindrical near-field acoustic holography, *J. Acoust. Soc. Am.*, **105**(4), 2269-2276, (1999).

2 Sarkissian A. Acoustic radiation from finite structures, *J. Acoust. Soc. Am.*, **90**(1), 574-578, (1991).

3 Cunefare K A. The minimum multimodal radiation efficiency of baffled finite beams, *J. Acoust. Soc. Am.*, **90**(5), 2521-2529, (1991).

4 Elliott S J and Johnson M E. Radiation modes and the active control of sound power, *J. Acoust. Soc. Am.*, **94**(4), 2194-2204, (1993).

5 WU Haijun. *Study on Computational Methods and Applications for Large Scale Acoustic Problems Based on the Fast Multiple Boundary Element Method*, Master of Science Thesis, Graduate Program in acoustics, Shanghai Jiaotong University, (2013).

6 Berkhoff A P. Sensor scheme design for active structural acoustic control, *J. Acoust. Soc. Am.*, **108**(3), 1037-1045, (2000).

7 NIE Yongfa. *Study on acoustic radiation modes theory and its applications*, Master of Science Thesis, Graduate Program in acoustics, Naval Engineering University, (2014).